JOINT EUROPEAN TORUS

JET–P(90)12

A. Gibson, P. Smeulders
and JET Team

The JET Project: A Review of Progress

The JET Project: A Review of Progress

A. Gibson, P. Smeulders
and JET Team*

JET-Joint Undertaking, Culham Science Centre, OX14 3DB, Abingdon, UK

** See Appendix 1*

Preprint of Paper to be submitted for publication in
Plasma Physics and Controlled Fusion

THE JET PROJECT : A REVIEW OF PROGRESS[1)]

by A.Gibson, P.Smeulders and the JET Team[2)]

ABSTRACT

JET has recently reached fusion relevant plasma parameters. An overview of the project is given showing the enhancements, that have been made and which have lead to the improved performance. The limits of the key parameters : n, β and τ_E will be presented and it will be shown that the central values of density n and temperature T are crucial. Ways to improve these will be discussed. The presentation of the presently obtained high fusion parameters will be followed by a discussion on results to be expected with D-T operation.

INTRODUCTION

a.Brief description of JET and its objectives.

The Joint European Torus (JET) is the largest single project under auspices of EURATOM. It is presently the largest tokamak in the world with a maximum current of 7 MA and a toroidal magnetic field of up to 3.45 T. The device has been described elsewhere (Bickerton et al. 1987, Bertolini et al. 1987, Gibson et al. 1988). The toroidal vessel, shown in fig.1, has a major radius of 2.96 m and a D-shaped cross-section of 2.5 by 4.2 m. The whole machine is about 15 m in diameter and 12 m high.

Its objectives are :
- to study the way the confinement and plasma properties scale as the dimensions and parameters approach those necessary for a fusion reactor;
- to examine and control the plasma-wall interactions and impurity influx in these conditions;
- to demonstrate effective heating techniques, capable of producing high temperatures in JET in the presence of the prevailing loss processes;

---

(1) This paper is a written version of a presentation made to the International Plasma Physics Conference New Dehli, November 1989

(2) Plasma Physics & Controlled Fusion **30**,(11),1390

- to study alpha-particle production, confinement and subsequent plasma interaction and heating, in short the physics of a reacting plasma.

b.The main enhancements for 1989.

In the year 1989 six major enhancements have been implemented.

1. A better control of the currents in the primary windings, that govern the plasma position and shape, is now available with the new booster amplifier and the digital feedback system. This has lead to stable more elongated plasmas of longer duration and a better coupling to the RF antennas. Plasma currents in limiter mode of up to 7 MA and in X-point operation with H-mode at up to 5 MA have been achieved.
2. To resist the forces of about 20000 kN in case of a disruption at maximum plasma current, vessel reinforcement rings have been installed, reducing the vessel movement in such a event by an order of magnitude to less than 2 mm.
3. The Carbon tiles on the inner wall and top X-point dump plates have been replaced by fibre reinforced Carbon. This has prevented fracture of the tiles by the high heat load and increased the reliability of the machine.
4. An automatic phase control of the Ion Cyclotron Resonant Heating (ICRH) system provides a low RF wave reflection coefficient at the antennas and therefore a more reliable coupling to the plasma and a more effective operation.
5. The penetration of the Neutral Beam Injection (NBI) at high plasma density has been improved by changing progressively more units from 80 to 140 kV Deuterium (D) injection.
6. A major improvement came with the introduction of Beryllium (Be) first as a coating and later as a limiter element in the machine.

Fig.2 shows the shape of the magnetic surfaces during a discharge with high plasma current and limiter operation. The plasma is limited by two belt limiters. Fig.3 shows a high current X-point configuration, in which case the last closed magnetic surface can be seen to be free from the two belt limiters.

The main plasma parameters : current I_p, temperature T_e, density n_e, confinement time τ_E and loop voltage V_l are shown as function of time for an Ohmically heated 7 MA discharge in fig.4. Fig.5 shows the same parameters for a 3 MA discharge, which has a current flat top of 33 s. It can be seen that

the plasma parameters vary little over this time, except for a 15 s. period in the middle of the pulse where low power NBI was applied. Other discharges had a heating pulse of in excess of 20 s. duration with 6 MW of applied power and T_e in excess of 6 keV.

c. The introduction of a Be environment and the main consequences.

Before the introduction of Be the effective plasma charge Z_{eff} was around 3 to 4 in operation with large additional heating (≥10 MW). The dominating impurities were Carbon C and Oxygen O and only a very small metal impurity content ($\approx 10^{-4}$ n_e). The D dilution was $n_D/n_e \approx 0.6$.In the first period of 1989 Be evaporation on the Carbon tiles was instituted on a regular basis. Typical wall coatings of ≈300 Å were obtained. The Be gettering essentially eliminates O, reduces the C content and improves of the D dilution to give $n_D/n_e > 0.8$. The Be coating of the limiter lasted for 1-3 pulses. In the course of these first pulses, the Be concentration in the plasma dropped from 3 to 0.5 %. The beneficial effects of the Be however persisted for many more pulses (>20).

The introduction of Be limiter tiles later in the year gave a further improvement. This has allowed for the first time in JET to get the H-mode of high-confinement regime [Tubbing et al.1989] with ICRH alone. H-modes can now be obtained in NBI, combined NBI and ICRH , and ICRH alone. Impurity levels as measured by the Z_{eff} values are low ($Z_{eff} \leq 2$) with a deuterium D dilution greater than 0.8. Radiated power losses are also strongly reduced.

A still further improvement of the plasma purity has been obtained in pellet fueled discharges. This has lead to highly peaked density profiles with $\hat{n}_e > 10^{20}$ m^{-3}, $Z_{eff} \approx 1.4$ and $n_D/n_e > 0.9$.

Another important feature of Be as wall material is that the operating range has been extended to both lower and higher plasma densities. The low densities are possible because of the strong pumping of the Be gettered walls and the higher densities are due to the increased density limit in purer plasmas.

In the operation at low density, high ion temperatures were obtained with $\hat{T}_i > 28$ keV and electron $\hat{T}_e > 12$ keV. In other discharges $\hat{T}_i$ and $\hat{T}_e$ were simultaneously in excess of 10 keV for several seconds. In the low density H-modes the density profiles are more peaked with $\gamma_n = \hat{n}_e/\langle n_e \rangle \simeq 1.5$, compared to previous high density H-modes with $\gamma_n \simeq 1$, presumably because of the central fueling due to good beam penetration.

On the high density side not only is the density limit increased by more than

a factor of 2, but in case of a disruption the subsequent recovery is much easier. The density limit is now no longer usually set by disruptions but by the appearance of strong asymmetries near the edge (so called MARFES). In low power H-modes energy replacement times have been measured, which are well in excess of 1 s. In general however no systematic difference in confinement is observed between discharges with beryllium walls and those with carbon walls.

2. THE QUANTITIES WHICH DETERMINE FUSION PERFORMANCE AND THE VALUES OBTAINED IN JET.

The quantities that determine in a thermal burning plasma the energy production and so the fusion performance are :

-the operating density
-the β-value (β is the ratio of plasma pressure to the magnetic field pressure)
-the dilution factor of the fuel ions due to impurities (i.e. reduction of n_D/n_e)
-the ion temperature
-the confinement time

Density.

The operating density in tokamaks is usually presented in the form given in fig.6. Each point represents the maximum obtained normalised density during a discharge with either Ohmic (OH), NBI, ICRH (RF) or combined heating. The broken lines marked by OH(C) and NBI(C) are the highest limits obtained in the previous campaigns with Carbon walls and limiters. There are clear improvements due to the Be limiters and Be coated walls. As explained previously the maximum density is no longer set by disruptions but rather by MARFES, there are indications that this limit increases with available heating power and it is likely that some kind of thermal instability at the plasma edge is involved. The limit at low q however is unchanged and is still set by major current disruptions. It corresponds to unstable plasma conditions at $q_\psi < 2$ for all densities.

β-value.

The β-value is important in JET since the fusion performance is related to the product $n.T.\tau_E \approx \beta.B^2.\tau_E$, furthermore the β value has important economic

implications in a fusion reactor. Troyon established computationally a quantitative estimate for the β limit in tokamaks for optimized profiles [Troyon et al. (1984)]. It turns out, that many experiments including JET follow this limit :

$$\beta_{Troyon} = 2.8\ 10^{-2}\ I/(B.a) \qquad [\ MA,T,m\ ]$$

In JET this limit can be obtained at a reduced toroidal field with the available heating power. The highest β-value of 5.5 % is obtained in JET is for a 2 MA, 1 T, X-point discharge with 11 MW of NBI (see fig.7). Usual operation in JET at 3.4 T occurs at β values of around half the Troyon value. Because the fusion power in a D-T plasma depends approximately on the square of the beta for a given magnetic field, an increase in fusion power by a factor 4 would be possible in JET within the β limit if the nT product could be increased (e.g. by increased heating or confinement). A very important result is that there is a soft degradation of the confinement as the β limit is approached, holding out the promise of a future automatic burn control mechanism. The degradation is related to the growth of toroidal low n-number kink modes, which have usually poloidally a m=1 structure near the plasma centre.

Dilution.

The main factors limiting the fusion performance in JET at the present are the confinement and the deuterium (D) dilution. The latter shows a strong dependence on the density of the plasma : the higher the density the lower the Z_{eff} and the higher n_D/n_e. Fig. 8 and 9 show the dependence of the measured Z_{eff} on the volume averaged density for OH plasmas and for those with additional heating between 7 and 15 MW. In each figure the results obtained in case of the carbon limiters are compared to those obtained after the introduction of Be limiters. In Ohmically heated plasmas Z_{eff} is in general lower at all densities and in particular at low values of $<n_e>$. The main improvement in plasmas with additional heating is that beryllium limiters permit operation at higher densities and at these higher densities lower values of Z_{eff} are consistently obtained.

However in case of X-point discharges, which have Carbon target plates, or discharges limited on the inner carbon wall Carbon still plays a dominant role at high power levels. This is due to an local overheating of the target tiles to above 1100 $^{\circ}$C at high power levels leading to large influxes of Carbon. The higher the heating power the shorter the time delay for the carbon influx. When the product of Δt and P reaches about 10 MJ, there is an escalation of the carbon influx leading to a strong dilution of the fuel and to a collapse

of the plasma temperature.
Measurements by Pasini et al [1989] in figs.10 and 11 show this effect. In fig.10 n_e is given as a function of time for 3 shots with different power levels. The sharp increase in n_e is a direct indication of the carbon influx. The onset of the influx can be delayed by sweeping the position of the plasma-wall contact over the carbon tiles, so that a wider distribution of the heat over the tiles occurs. In fig.11 this can be seen for discharge 19387, for which the vertical position has been changed from -2 to +3 cm thus sweeping the interaction area and giving an extra delay of around 0.5 s. This demonstrates that if one can devise an X-point target chamber, which can accept the heat flux without excessive wall temperatures the plasma can be kept clean and undiluted.

Ion Temperature.
The reason why such high powers above the ohmic level are applied is of course to obtain ion temperatures of thermo-nuclear interest. Indeed very high ion temperatures have been reached in JET and $\hat{T}_i$ depends nearly linearly on $P_t/\hat{n}_e$, see fig.12.

Confinement Time.
The increase in power however affects another important fusion parameter τ_E. The confinement degrades with increasing power level. In case of limiter plasmas (i.e. plasmas bounded by the belt limiters or by the inner wall) the scaling of the confinement time in JET can be represented by the so-called Goldston scaling [Goldston et al. 1984]

$$\tau_E^G = 3.7\ 10^{-2}.H.I_p.(P_t-\dot{W})^{-0.5}.R^{1.75}.a^{-0.37}.(b/a)^{0.5} \quad [s,MA,MW,m] \qquad (1)$$

with the multiplier H equal to 1 for so called L-mode confinement. The dependence of τ_E on the effective power (total input power minus rate of change in plasma energy ($\dot{W}_p$)) for various plasma currents is given in fig.13. Good agreement between the measured values and the scaling (with H=1) within the spread of the experimental data exists.It should be noted however that other scaling laws, in which the plasma energy shows an offset linear dependence on power and which have a more physical basis [Rebut et al.(1988)], also lead to an equally good fit to the experimental data.
In the case of X-point discharges a high confinement regime or H-mode first discovered in ASDEX [Wagner et al.1982] can be obtained, these discharges show agreement with the scaling (1) with H around 2 (fig.14).

THE IMPORTANCE OF PEAKED PROFILES FOR FUSION PERFORMANCE

The cross-section for D-T fusion $\langle\sigma v\rangle_{DT}$ is approximately proportional to T_i^2 for ion temperatures T_i between 7 and 25 keV . Profiles of $n(\rho)/\hat{n}$ and $T(\rho)/\hat{T}$, that have a $(1+\rho^2)^{\alpha}$ dependence on $\rho=r/a$, then lead to the following α-particle power in a thermal D-T plasma with $n_D=n_T=\frac{1}{2}n_i$ [Gibson et al.1988]:

$$P_\alpha(\text{thermal}) \simeq 7.7\ 10^{-38}.(2\alpha+1)^{-1}.\hat{n}_i^2.\hat{T}_i^2.V. \qquad [W,m^{-3},keV] \qquad (2)$$

where $\alpha = \alpha_n + \alpha_T$ and V is the plasma volume. For most JET discharges $\alpha \simeq 1.6 \pm 0.7$, except in the case of pellet fueled plasmas where $\alpha \approx 4$.
The ratio of P_α to the total power losses ($P_L=W/\tau_E$) follows for $T_e = T_i$:

$$Y = P_\alpha/P_L = 3.3\ 10^{-22}.(\alpha+1).(2\alpha+1)^{-1}.\hat{n}_i.\hat{T}_i.\tau_E \approx C.X \quad [m^{-3},keV,s] \qquad (3)$$

The parameter $X = \hat{n}_i.\hat{T}_i.\hat{\tau}_E$ is the fusion product. C is a weak function of α and varies only by ±10% around 2×10^{-22} if α changes from 1 to 4. The fusion parameter Y is thus directly related to the fusion product X and in the approximation where C is constant Y and X are directly proportional. The true relation using the actual D-T fusion cross-section and typical profiles is shown by the shaded bands on fig.16.
The expression $X = \hat{n}_i.\hat{T}_i.\tau_E = \gamma_n.\gamma_T.\bar{n}_i.\bar{T}_i.\tau_E$ can be written as :

$$X = 1.06\ 10^{20}.P_L.\tau_E^2.\gamma_n.\gamma_T/(R.a.b) \qquad [MW,s,m] \qquad (4)$$

where $\gamma_n = \hat{n}/\bar{n}$ and hence $\gamma_n=\alpha_n+1$ with similar relations for γ_T. The fusion product is roughly proportional to the product of the peaking factors of the temperature and density profiles. This product is shown in fig.15 for limiter and L-mode discharges and separately for H-mode discharges. H-mode discharges usually possess flat to hollow density profiles with $\gamma_n \simeq 1$, although as can be seen the product $\gamma_n.\gamma_T$ can reach values ≈ 3 even at low q_ψ in certain discharges. Substituting the Goldston form for τ_E gives :

$$X \propto H^2.\gamma_n.\gamma_T.I_p^2.(R/a)^{2.5}.a^{-0.24} \qquad (5)$$

For a given device the maximum of X and hence of Y is determined and obtained by maximising: $H^2.\gamma_n.\gamma_T.I_p^2$. This means H-modes, peaked profiles and high current discharges.

FUSION PERFORMANCE IN JET

The fusion performance obtained in JET is shown in fig.16. The product X of $\hat{n}.\hat{T}.\tau_E$ is shown as a function of T_i for various plasma currents in H-modes, pellet and low density high $T_i$discharges. The highest $\hat{n}.\hat{T}.\tau_E$ values approach those, that are required for break-even with Q=1 in D-T plasma. Q is the ratio of the total fusion power (α-particles and neutrons) over the total power input for a plasma in steady state, Q is approximately 5×Y. The actual fusion power measured in these D discharges is shown in the form of the Q_{DD} versus volume averaged density in fig.17. The highest Q_{DD}values are obtained at moderate densities and high ion temperatures in H-modes. The highest H-mode values are twice those in L-mode.

The time evolution of a discharge with such high Q_{DD} values is shown in fig.18. The top traces show the time development of central ion temperature together with the neutron yield. Also shown are the total plasma energy as measured by the plasma diamagnetism and the volume averaged density. The break in the slopes of T_i, Y_n, W_{dia}, $<n_e>$ in time, mark the point where the carbon influx becomes important shortly before 11.5 s. The X-point discharge is in a H-mode state over nearly 1 s. as can be seen from the D_α signal. The bottom traces are the total NBI power and the radiation losses measured in time. Despite the large C influx radiation losses never become dominant in this discharges. The main fusion relevant parameters for this discharge #20981 are summarised in table I.

DOUBLE NULL H-MODE PULSE 20981, B_φ = 2.8 T, I_p = 4 MA

Plasma Parameters at t=11.4 s

$\hat{T}_i$	= 22 keV	$\langle T_i \rangle$	= 5.8 keV
$\hat{T}_e$	= 8.6keV	$\langle T_e \rangle$	= 5.2 keV
W_p	= 10 MJ	$\dot{W}_p$	= 9. MW (non-steady
$\hat{n}_D$	= 3.7 10^{19} m^{-3}	$\langle n_D \rangle$	= 3.2 10^{19} m^{-3} state)
$\hat{n}_D/\hat{n}_e$	= 0.9	$\langle n_D/n_e \rangle$	= 0.8
$\hat{Z}_{eff}$	= 1.4	$\langle Z_{eff} \rangle$	= 1.9
Y_n	= 3.7 10^{16} n/s	P_t	= 17 MW
τ_E	= 1.1 s		

D-D Observed Fusion Parameters

Q_{DD} = 2.5 10^{-3} (>1.7 10^{-3} for 0.5 s)

P_{fusion} = 43 kW (D-D)

$\hat{n}_i \hat{T}_i \tau_E$ = 9. 10^{20} m^{-3} keV s (>3.10^{20} for 0.5 s)

Equivalent D-T Parameters

Calculated (TRANSP and JETTO code)
for 140 kV injection of beams

Q_{DT}	= 0.7	(> 0.5	for ≈0.8 s)
Q_{th}	= 0.13	(plasma-plasma	)
Q_{bp}	= 0.57	(beam-plasma	)
P_{fusion}	≃ 12 MW	(> 8 MW	for ≈0.8 s)
P_α	≃ 2.4 MW	(> 1.6 MW	for ≈0.8 s)
P_α/P_L	≃ 23 %	(> 15 %	for ≈0.8 s)

TABLE I

The discharge has been studied by a plasma simulation code JETTO [Cenacchi et al.1988] and by the transport code TRANSP [Balet et al.1989]. First good agreement between some selected predicted data and the corresponding measurements was established i.e. the total neutron rate and the plasma energy content and Z_{eff} as function of time for both codes. In case of the simulation code the calculated density and temperatures profiles were in reasonable agreement with the measured profiles for pure deuterium plasmas. Then the fuels in the plasma and in the neutral beams (with an acceleration energy of 140 kV. and the correct species mix) were changed to various mixtures of D-T. The results obtained by the two quite different codes were in very good agreement. The results are shown in table I for a 50-50 D-T plasma mixture and 140 kV deuterium beams for TRANSP and 50-50 D-T beams for JETTO. A nearly identical result was obtained in TRANSP by simulating the neutral injection of 140 kV beams into an initial tritium plasma.

5. EXPECTED BEHAVIOUR OF α PARTICLES IN JET BASED ON FUSION PRODUCTS GENERATED IN PRESENT D-D AND D-He^3 EXPERIMENTS

Already in 1988 α-particle experiments [Start,1989] were carried out in JET. This year ICRH of a minority ^{3}He distribution in a D background plasma accelerated the He ions to energies of 1 to 5 MeV. The total energy stored in these particles reached 2.4 MJ, which represented about 50 % of the total plasma energy and is higher than in earlier experiments by $\approx$ 1 MJ due to a better control of density with the Be walls. The increased D-^{3}He fusion power from 60 to 100 kW also reflects the improvement of n_D/n_e from $\leq$0.6 to $\geq$0.8. Fig.19 gives the total fusion power due to the D-^{3}He fusion process in discharges with carbon and with beryllium walls as a function of the ICRH power. The total fast ^{3}He minority energy content in these discharges is fully explained by the coupled ICRH power and classical slowing-down of the fast particles which takes places mainly on the electrons.
Because of the similarity between the fast ^{3}He particles and the α-particles it can be concluded [Sadler et al.1989] that α-particle slowing down is classical and the confinement of the α's in JET will be sufficient to give α-particle heating during the D-T phase. The comparison of plasma and α-particle parameters measured in JET and those for the future D-T operation and for an ignited next step are given in table II [Bickerton, 1988].

D - ^{3}He experiments (^{3}He minority - 1-5 MeV)			
parameter	Achieved JET	JET (Q=1)	Ignited ITER
$\hat{n}_f / \hat{n}_e$	10^{-2}	10^{-3}	10^{-2}
$\hat{\beta}_f$ (%)	1	0.6	2
E_f (MeV)	1-5	2	2
v_f / v_A	1-2	2	2.8
$p_\perp / p_\parallel$	10-50	1	1
P_f / P_L	0.8	0.17	1
r_ϑ / a	0.2-0.4	0.3	0.07

TABLE II

The only major difference between the parameters in α-particle simulation experiments in JET and those foreseen for the future lies in the large velocity space anisotropy of the high energy of ^{3}He particles generated by ICRH.
The α-particle behaviour in JET has also been monitored through the Triton burn-up. The T is produced by the D-D reaction and can be monitored through the 14.1 MeV neutron production. It turns out that the burn up is classical within a 20 % margin [Conroy et al.1989]

THE FUTURE DIRECTIONS OF THE JET PROGRAMME

A very important task for JET in the future will be to demonstrate effective methods of impurity control, of plasma fueling and particle exhaust.
JET will concentrate on the reactor relevant X-point operation. The addition of an internally pumped divertor for impurity control is under discussion.
The design is believed to be capable of handling the expected power loads, so that large impurity influxes can be avoided. Fig.20 shows a cross-section in a radial plane of the proposed configuration [Rebut et al.1989]. Projection of magnetic field lines in the separatrix region on to this plane are also shown. The lower part of the figure is enlarged and displayed in fig.21. Field lines in the X-point region just above the internal divertor coil can be seen. The dump plates will be water cooled to allow for long pulse operation. To the right of the divertor coil are large cryopanels for the pumping of the

divertor.
Fig.22 shows the proposed JET programme now under discussion, it extends to the end of 1996, so that impurity control studies in the new configuration can be carried out and then exploited to demonstrate sustained plasmas with fusion relevant parameters. The demonstration and investigation of α-particle behaviour and plasma heating in a D-T mixture remains the final goal of the programme.

CONCLUSIONS

JET has operated with up to 7 MA of plasma current with a total plasma volume of 120 m^3. Operation has taken place in full aperture and in X-point discharges. Some 13 MJ of plasma energy has been created. The best operation has produced a fusion product $X = \hat{n}_i.\hat{T}_i.\tau_E = 7 \Rightarrow 9\ 10^{20}\ m^{-3}keV\ s$, with $\hat{T}_i = 22$ keV. The observed Q_{DD} of 2.5 10^{-3} would correspond to a Q_{DT} of about 0.8 for 140 kV Neutral Beam Injection into a D-T mixture with similar plasma conditions, Q_{DT} being calculated to be in excess of 0.5 for more than 0.5 s.

Other operation has separately produced confinement times in excess of 1.5 s, ion temperatures in excess of 28 keV and central electron densities in excess of 4 $10^{20}m^{-3}$. These parameters are already commensurate with those required in the plasma of a reactor.
These parameters imply that if a D-T mixture were to be introduced into JET today the fusion power would be more than 8 MW, with an α-particle heating in excess of 1.6 MW for more than 0.8 s, the ratio of P_α/P_{Loss} would be over 20 % although the plasma would be far from steady state.

Some further improvement is to be expected in the next two years with further refinement of operation techniques and with the installation of better X-point target plates and Lower Hybrid Current Drive (to give some control of the current density distribution).
The duration of the good fusion conditions in JET is at present set by the influx of Carbon impurities due to local overheating of sections of the limiting wall surfaces or target plates. A new phase is planned for JET to demonstrate a reactor relevant solution to this problem leading to sustained production of a few megawatts of α-particle heating by 1996. The scene will then be set for the construction of a fusion reactor demonstration device.

REFERENCES

BALET B.,STUBBERFIELD P.(1989) JET Report R(89)05

BERTOLINI E.,HUGUET M. et al. Proc. 12th Symposium on Fusion Engineering (Monterey, USA) 1987 (also JET Report P(87)52)

BICKERTON R. et al.(1987) Plasma Physics and Controlled Fusion **10A**,1219

BICKERTON R. et al.(1988) Proc. 12th Int.Conf.on Plasma Phys.and Contr. Nucl. Fusion Research, Nice, IAEA-CN-50

CENACCHI G.,TARONI A.(1988) JET Internal Report IR(88)03 "JETTO: A Free-boundary Plasma Transport Code (Basic Version)"

CONROY S. et al.(1989) Proc. 16th Eur.Conf.on Contr.Fusion and Plasma Physics, Venice (also JET Report P(89)03)

GIBSON A. et al.(1988) Proc. 15th Eur.Conf.on Contr.Fusion and Plasma Physics, Dubrovnik (also JET Report P(88)26)

GOLDSTON R.(1984) Proc. 11th Eur.Conf.on Plasma Phys.and Contr. Nucl. Fusion Aachen, 6(1984)87

PASINI D. et al.(1989) "Observations on the Erosion of Carbon at High Temperatures in JET", Topical Meeting on High Temperature Erosion of Graphite in Plasmas, Princeton Plasma Physics Laboratory, July 25-27, 1989. To be published as a DOE report on Plasma Material Interaction and High Heat Flux Test Group. Editor R.E.Nygren.

REBUT P. et al.(1988) Proc. 12th Int.Conf.on Plasma Phys.and Contr. Nucl. Fusion Research, Nice, IAEA-CN-50

REBUT P. et al.(1989) 13th Symposium on Fusion Engineering, Knoxville USA (also JET Report P(89)79)

SADLER G. et al.(1989) IAEA Technical Committee Meeting on α-particles, Kiev, USSR (also JET Report P(89)77)

START D. et al.(1989) IAEA Technical Committee Meeting on α-particles, Kiev, USSR (also JET Report P(89)78)

TROYON F.,GRUBER R. et al. Plasma Phys. Controll. Fusion **26**(1984)209

TUBBING B. et al.(1989) Bulletin of the American Phys.Soc.**34**,9,2055

WAGNER F. et al.(1982) Proc. 9th Conf.on Plasma Phys.and Contr.Nucl.Fusion Research, Baltimore, IAEA

SYMBOLS

The following is a list of symbols used in the text

Geometry

R	Major radius of the plasma
r	Minor radius of the plasma surfaces in the horizontal plane
a	Minor radius of the plasma edge in the horizontal plane
b	Minor radius of the plasma edge in the vertical plane
A	Area of plasma cross-section in the poloidal plane
V	Plasma volume

Magnetic field

B_φ	Toroidal magnetic field
B_ϑ	Poloidal magnetic field
I_p	Plasma current
q_c, q_{cyl}	Cylindrical safety factor ($q_c^{-1} = \pi R I_p / 5 A B_\varphi$)
q_ψ	True safety factor related to actual pitch of magnetic field lines at the plasma boundary

Atomic

H,D,T	Hydrogen isotopes
^{3}He	Helium-3 isotope
Be,C,O	Beryllium, Carbon and Oxygen plasma impurities
Z_{eff}	Effective plasma charge due to hydrogen and impurity concentrations

Power and Energy

W, W_p	Plasma energy content
W_{dia}	Plasma energy content based on the diamagnetic measurements
P_t,P_{tot}	Total plasma power input
NB, NBI	Neutral Beam Injection
ICRH,RF	Ion Cyclotron Resonance Heating or Radio Frequency heating
OH	Ohmic Heating
V_l	Loop voltage over the torus related to the plasma current I_p
P_α	α-particle heating power
P_L	Plasma power losses ($P_L = P_t + P_\alpha - dW/dt = W/\tau_E$)

P_{eff}	Effective plasma power input ($P_{eff} = P_t - dW/dt$)
P_{fus}	Total fusion power (for D-T reactions : $P_{fus} \simeq 5 \times P_\alpha$)
P_f	ICRH power coupled to the fast ions
τ_E	Energy confinement time ($\tau_E = W/P_L$)
H	Multiplier in τ_E scaling for H-modes
Q	Ratio of P_{fus} over P_t
Q_{DD}	Q for D-D reactions
Q_{DT}	Q for D-T reactions

Plasma

$\hat{T}_{e,i}$	Central electron and ion temperature
$\hat{n}_{e,D,I}$	Central electron, deuterium and ion density
$\bar{n}_e$	Line-averaged electron density
$<n_e>$	Volume-averaged electron density
p	Plasma pressure : 3nkT
$p_{\perp,\parallel}$	Pressure perpendicular and paralel to the magnetic field
β	Ratio of plasma pressure over magnetic pressure ($B^2/2\mu_0$)
$\beta_{\varphi,\vartheta}$	β with respect to toroidal and poloidal magnetic field
β_f	β_φ of the fast plasma ions
v_f	Average velocity of fast ions
v_A	Alfven velocity
E_f	Average energy of fast ions
Y_n	Total neutron yield
D_α	Measured D_α light emission by the neutral deuterium atoms

Profiles

$\alpha_{n,T}$	Peaking index for density and temperature profiles
$\gamma_{n,T}$	Another measure of profile peakeness : $\gamma = \alpha+1$ ($\gamma_n = \hat{n}/<n>$)

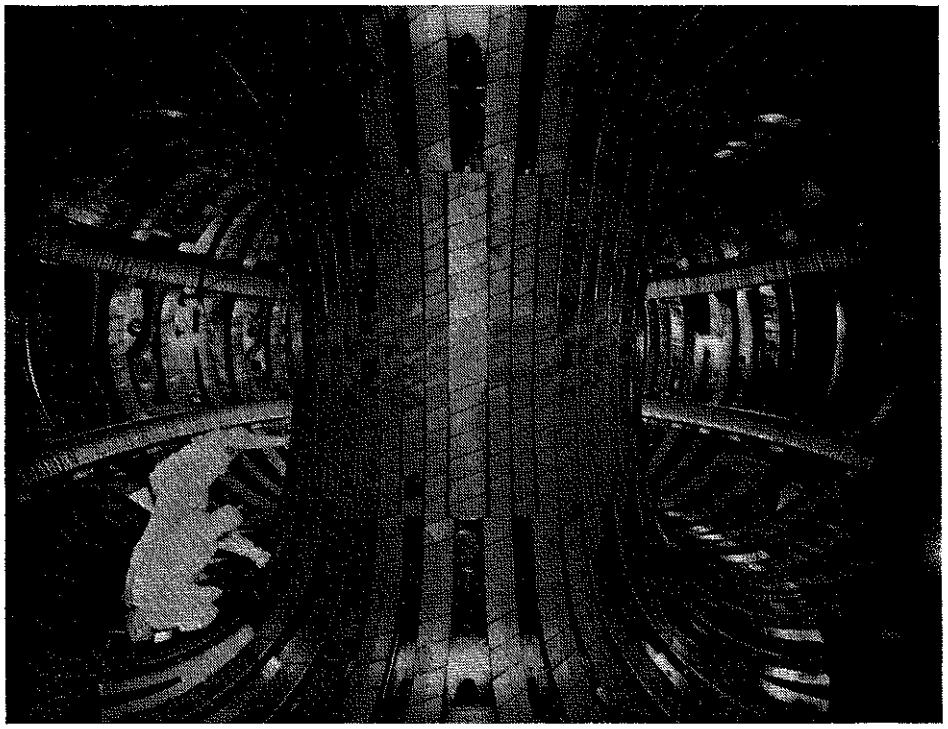

Fig.1. The interior of the vacuum vessel with in the centre the central inner wall covered with carbon tiles. Visible are the two limiter belts above and below the torus mid plane and three of the Ion Cyclotron Resonance Heating (ICRH) antennas between the two belts.

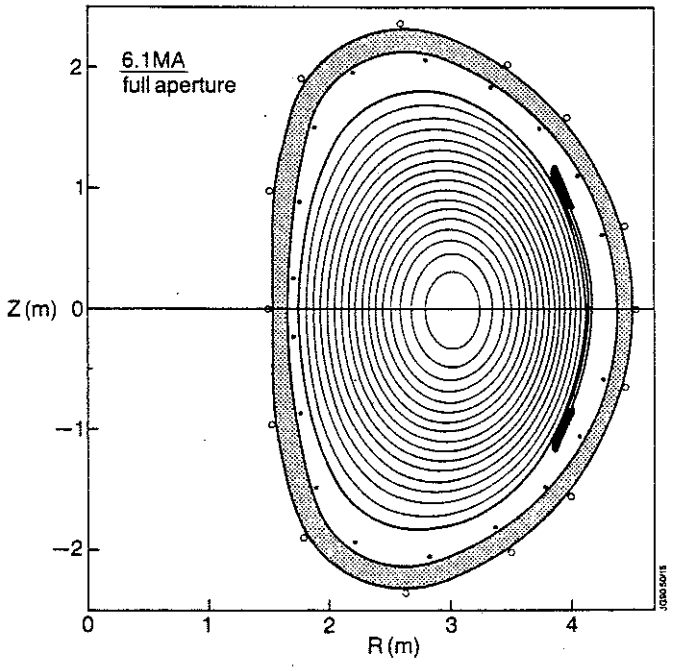

Fig.2. Contours of the plasma cross-section of shot #15750 in a full aperture limiter configuration, a plasma current of 6.1 MA and a safety factor q_ψ of 3 (q_{cyl}= 2.1). The gray D-shaped ring surrounding the plasma represents the vacuum vessel. The flat black areas are the two belt limiters catching the last magnetic plasma surface. The ICRH antennas are shown as the two lines connecting the two belts. The symbols o and * represent the magnetic pick-up coils and flux loops used to calculate the equilibrium surfaces.

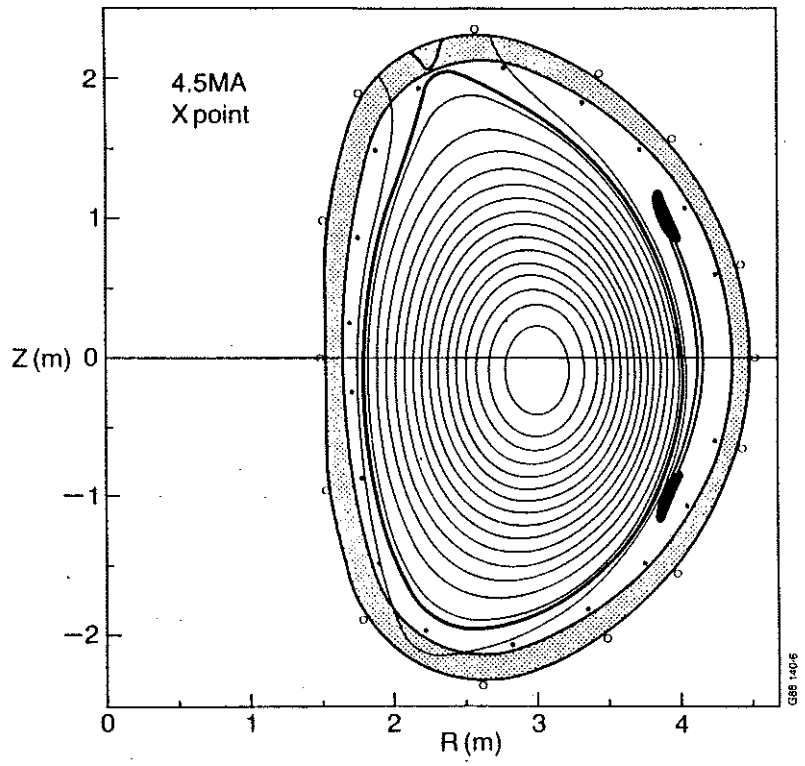

Fig.3. The plasma cross-section for a X-point configuration (shot #15494), with a plasma current of 4.5 MA and $q_{cyl} = 3.1$.

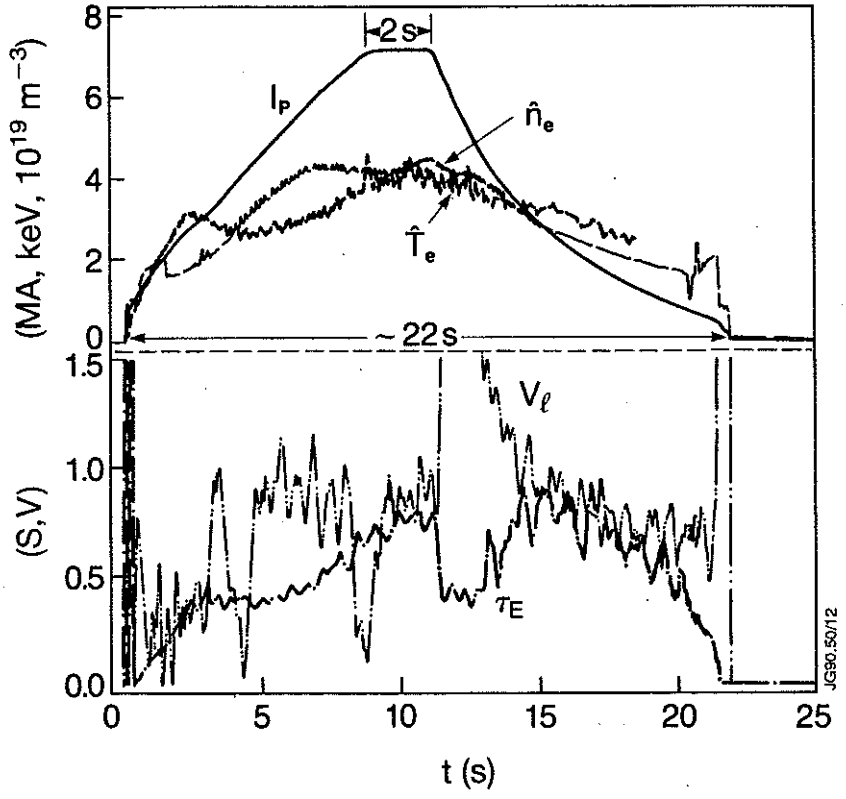

Fig.4. Time evolution of a 7 MA discharge together with its central $\hat{T}_e$ (- -) and $\hat{n}_e$ (— —) with below the confinement time τ_E (-·-) and loop voltage V_l on axis (-· ·-). A flat top of 2 s is achieved during which $\hat{T}_e = 4$ keV , $\hat{n}_e = 4.3\ 10^{19}$ m^{-3} , $V_l = 0.9$ V and $\tau_E = 0.6$ s.

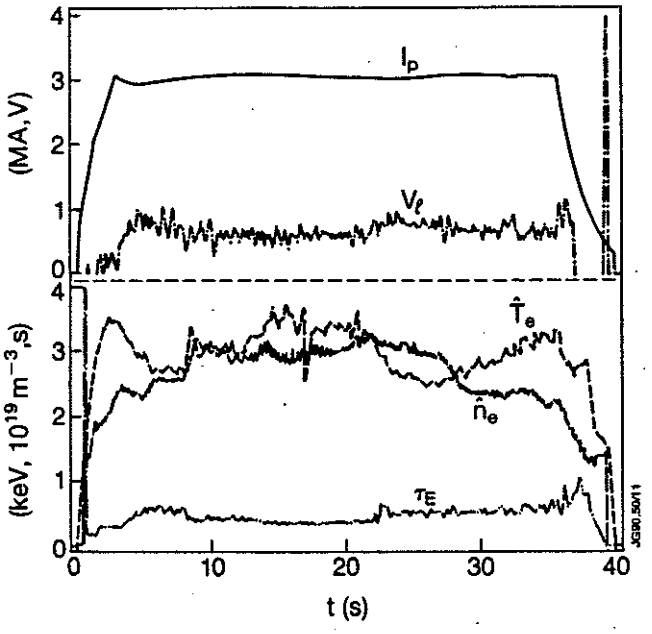

Fig.5. Time evolution of a long pulse discharge with a 33 s current flat top and a 15 sec long NB injection pulse of 4 MW from 8 to 23 s. From top to bottom plasma current I_p, loop voltage V_ℓ on axis (-·-), central electron temperature $\hat{T}_e$ (- -), central electron density $\hat{n}_e$ and confinement time τ_E (-·-) are shown as function of time.

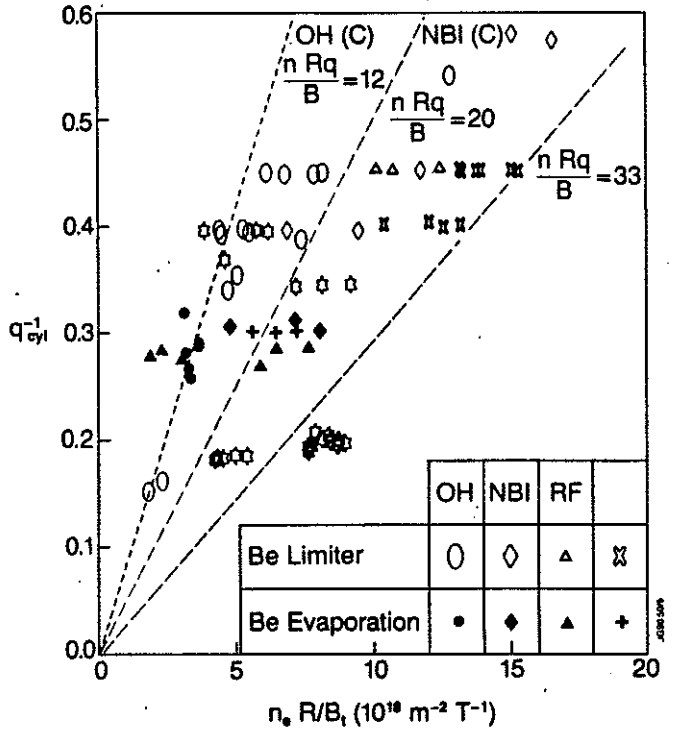

Fig.6. The operating density range for JET shown as normalised current $q^{-1}_{cyl} = \pi R I_p / 5 A B_\varphi$ [m,MA,m^2,T] versus normalised density $n_e R/B_\varphi$ [m^{-3},m,T]. The broken lines with nRq/B = 12 and 20 resp. represent the maximum density values obtained before the introduction of Beryllium into the vacuum vessel for ohmic heating (OH(C)) and for Neutral Beam heating (NBI(C)). The symbols are the maxima obtained after the introduction of Be for various heating scenarios.

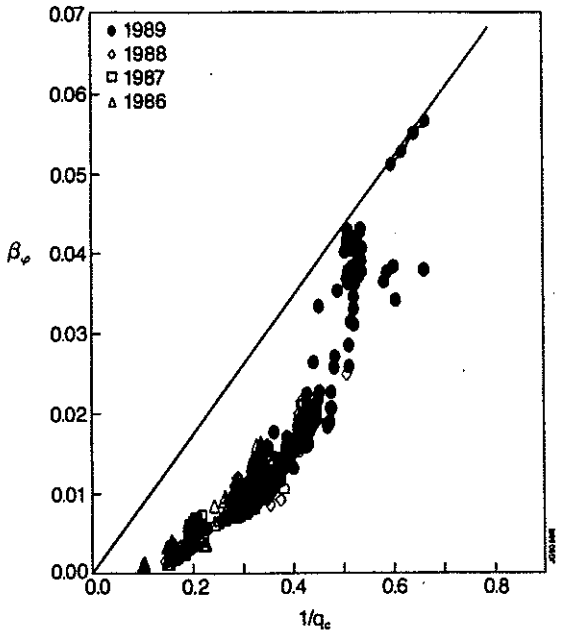

Fig.7. The maximum toroidal beta ($\beta_\varphi = 2\mu_o\langle p\rangle/B_\varphi^2$) as function of the normalised current $q_c^{-1} = \pi RI_p/5AB_\varphi$ for all JET discharges from 1986-1989 with the poloidal beta $\beta_\vartheta > 0.4$. The line is approximately the Troyon limit : $\beta_{Troyon} = 0.028\ I_p/aB_\varphi$ [MA,m,T]. The highest β of 5.5 % is obtained in a 2 MA, Double-Null H-mode discharge at 0.9 T with $\hat{T}_e = 3.7$ keV, $\hat{T}_i = 6.3$ keV, $\hat{n}_e = 3\ 10^{19}\ m^{-3}$, $P_{NB} = 11$ MW, deuterium injection in a hydrogen plasma.

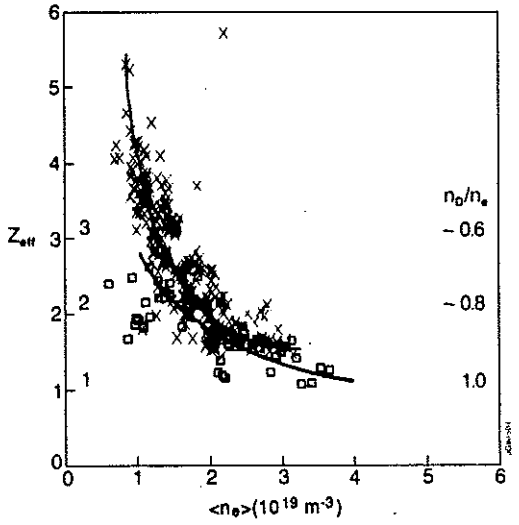

Fig.8. Measured Z_{eff} values as function of volume averaged electron density $\langle n_e\rangle$ in ohmically heated discharges for carbon limiters (x) compared to the values obtained in discharges with beryllium limiters (□). The values are taken at the time of maximum energy content for ≈ 3 MA, ≈ 3.2 T, limiter D plasmas. $Z_{eff} = 3$ corresponds in the case of the carbon limiter plasmas to a deuterium concentration $n_D/n_e \simeq 0.6$ as indicated in the figure. Z_{eff} in case of Be limiters and low densities is appreciably reduced as compared to C limiters.

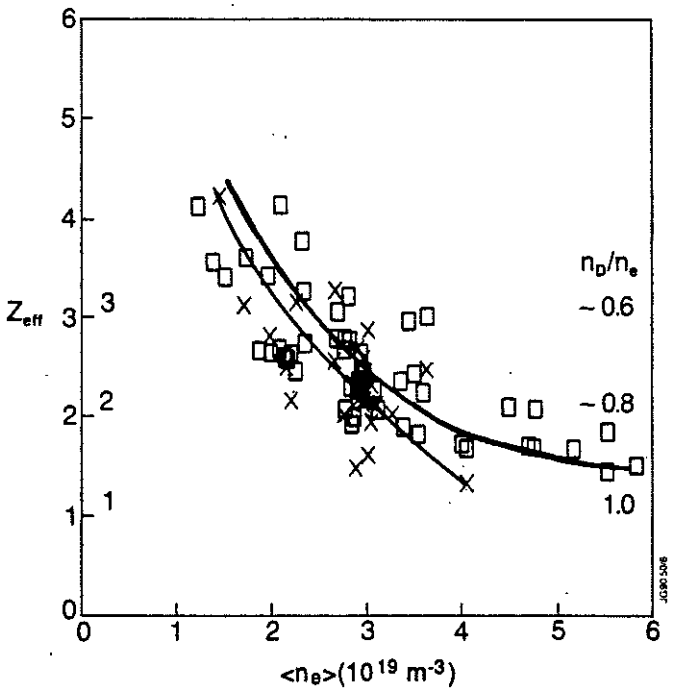

Fig.9. Z_{eff} versus $<n_e>$ for C (x) and Be (□) limiter plasmas with additional heating power between 7 and 15 MW. As in fig.8 the lines show again the trend of Z_{eff} to decrease with increasing n_e or increasing gas-puffing. In the beryllium limiter case a very high gas-puffing is required to reach high densities. This results in plasmas with higher densities and high deuterium concentrations with low Z_{eff} values.

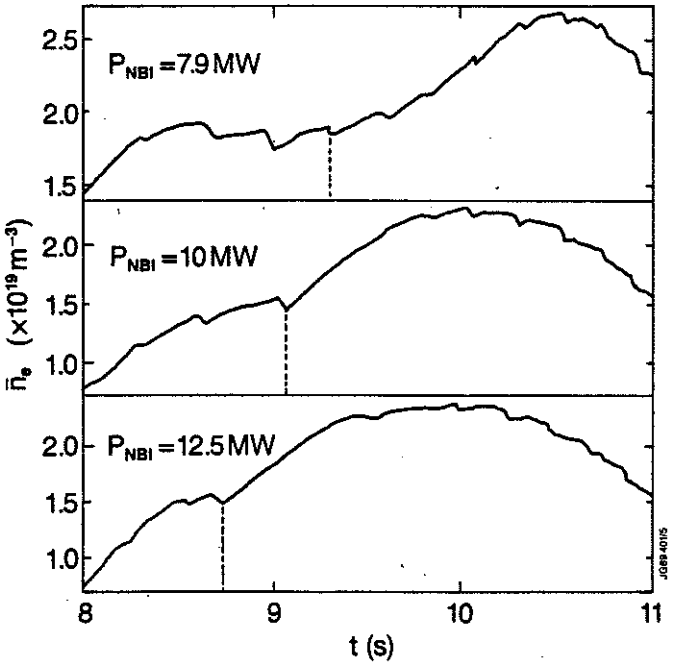

Fig.10. Effect of varying the additional heating power P on the onset of the high carbon influx. The onset is readily visible on the line average electron density $\bar{n}_e$ for the discharges #19388, #19385 and #19401, it is marked by the vertical broken lines. The product $P.\tau_{onset}$ is about 10 MJ : the higher the heating power the shorter the time delay for the carbon influx.

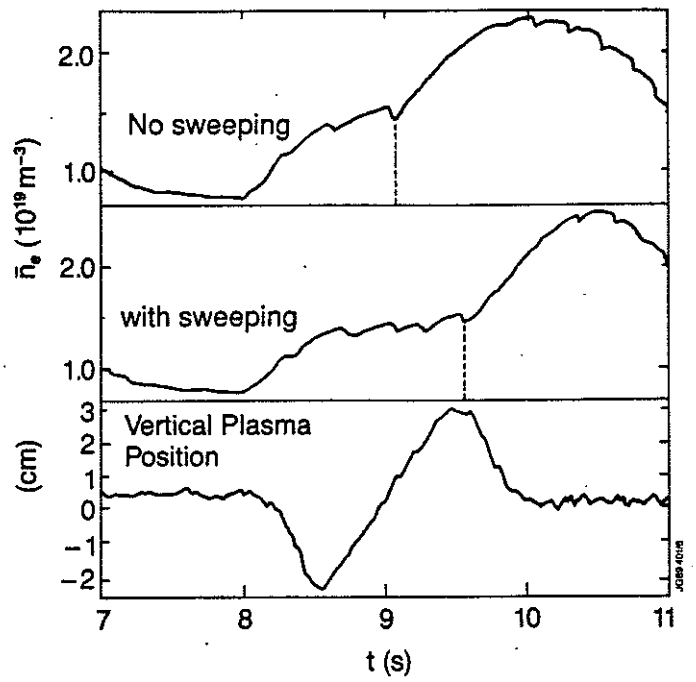

Fig.11. The dependence of the onset of the carbon influx on the sweeping of the plasma contact position on the inner wall limiter. Comparison of a discharge #19385 without and with sweeping #19387. Sweeping of the plasma on the inner wall delays the carbon influx by a few hundreds of ms.

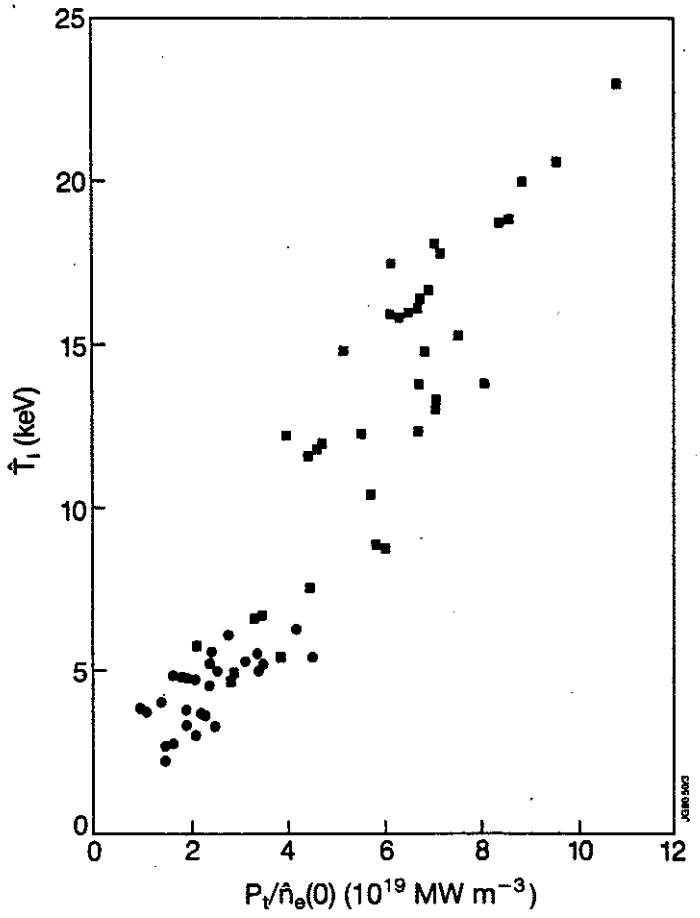

Fig.12. The dependence of the central ion temperature $\hat{T}_i$ on the ratio of the total input power P_t to the central electron density $\hat{n}_e$.

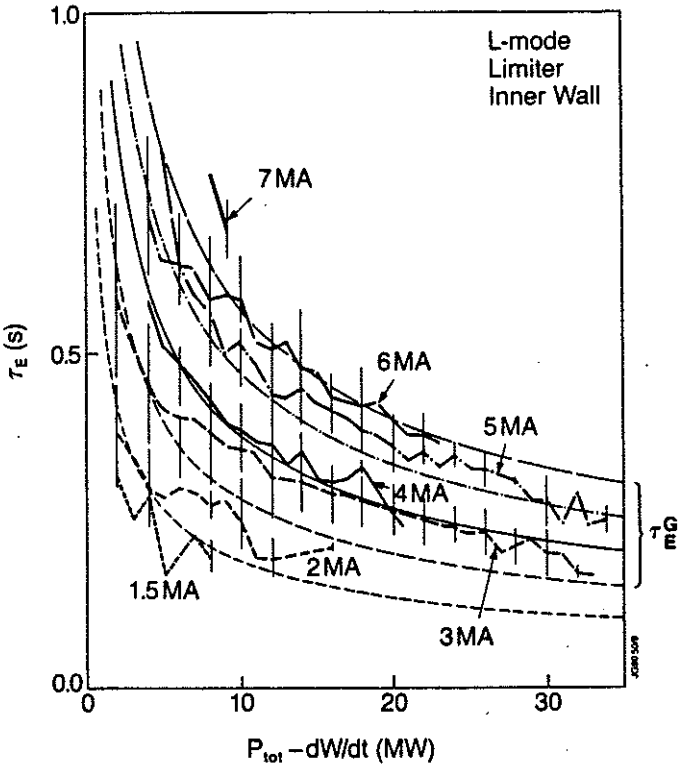

Fig.13. Energy confinement time τ_E as function of the effective input power $P_{eff} = P_{tot} - dW/dt$ for various limiter, inner-wall and L-mode plasmas with currents of 1.5, 2, 3, 4, 5, 6 and 7 MA. The smooth curves are the Goldston scaling τ_E^G for each current. The bars represent the scatter of the data being ± one standard deviation.

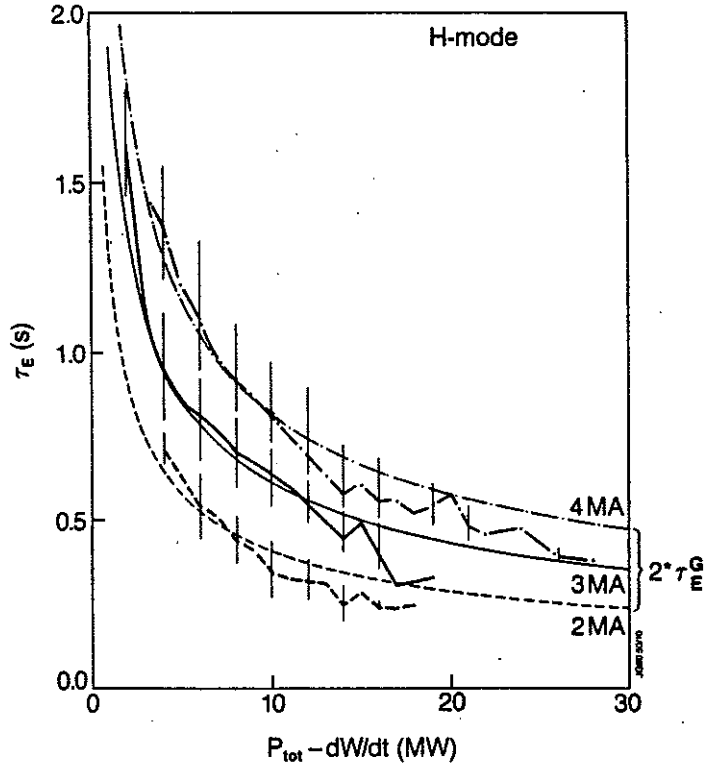

Fig.14. τ_E as function of P_{eff} for 2, 3 and 4 MA H-modes. The smooth curves are twice the Goldston scaling τ_E^G for each current.

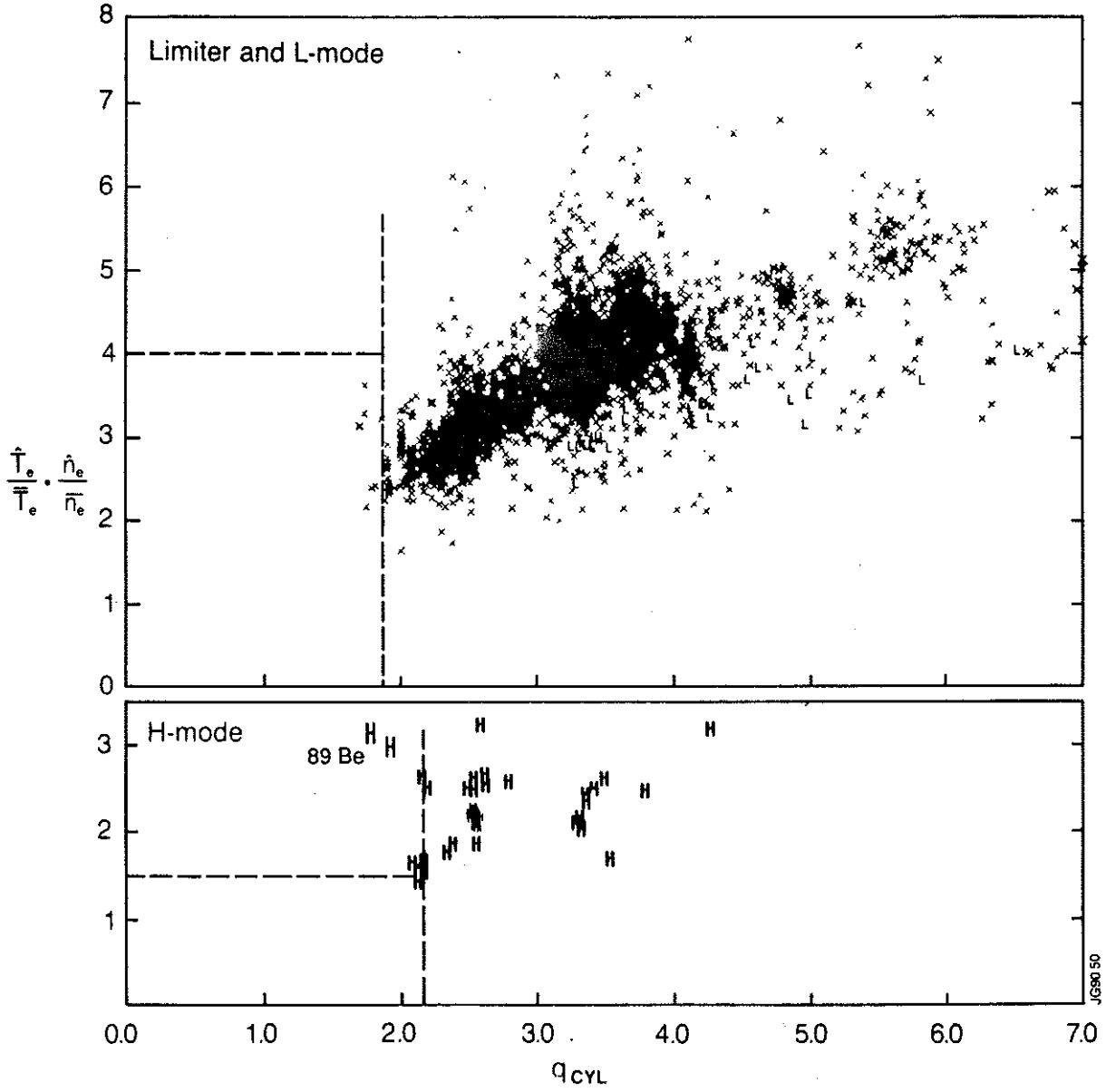

Fig.15. Profile peaking factor $\gamma_T.\gamma_n = \hat{T}_e/\bar{T}_e.\hat{n}_e/\bar{n}_e$ as function of q_{cyl} for limiter, L-mode and H-mode data. In H-mode discharges the density profiles are generally flat to hollow with $\gamma_n \simeq 1$ and therefore the product of the γ's is considerably less. The hot-ion H-modes with deep central beam fueling are indicated by (Be 89) and have $\gamma_n\gamma_T \approx 3$, these discharges have the highest neutron rates.

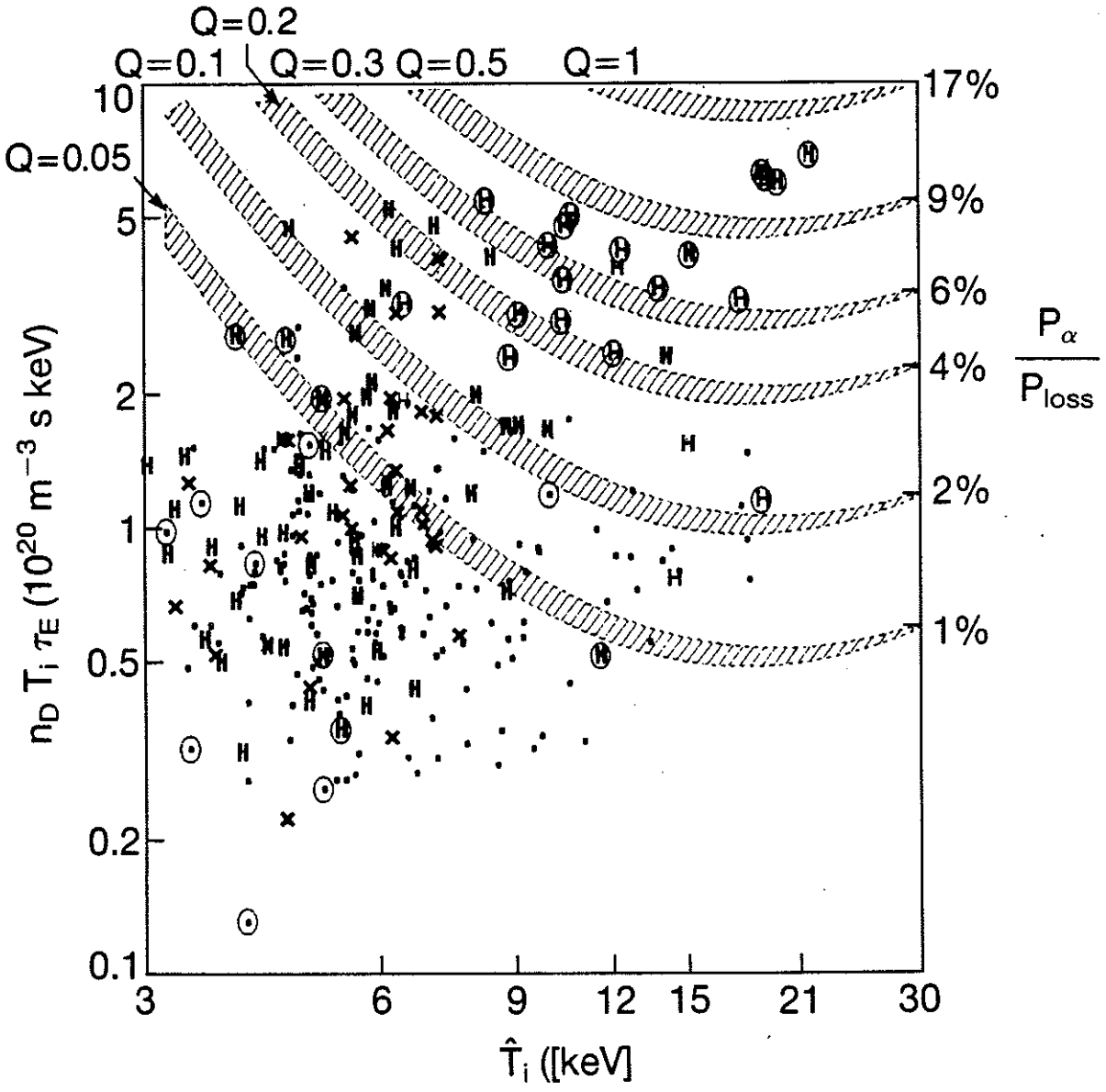

Fig.16. The product of $\hat{n}_D.\hat{T}_i.\tau_E$ as function of $\hat{T}_i$ for I_p between 2 and 6.5 MA in H-modes (H) , pellet (x) (including H-modes with pellets) and other (■) discharges (including low density high T_i discharges). The experimental points are averaged over 0.2 s. Also indicated in the graph are shaded bands of constant P_α/P_{Loss} for thermal 50:50 D-T plasma. In steady state these bands also correspond to the Q_{DT} shown. The width of the bands covers a range of profiles and dilutions in this case from α_n=0.5, α_T=1.5 with n_D/n_e=1 to α_n=0, α_T=3 with n_D/n_e=0.8 and the addition of a 20% temperature pedestal. It will be seen that the Q values especially at higher T_i are insensitive to these variations. The encircled points are at non-steady state with $\dot{W}/P_T$>0.3. For these points the shaded bands represent the thermal component of P_α/P_{Loss}, but not of course the thermal Q.

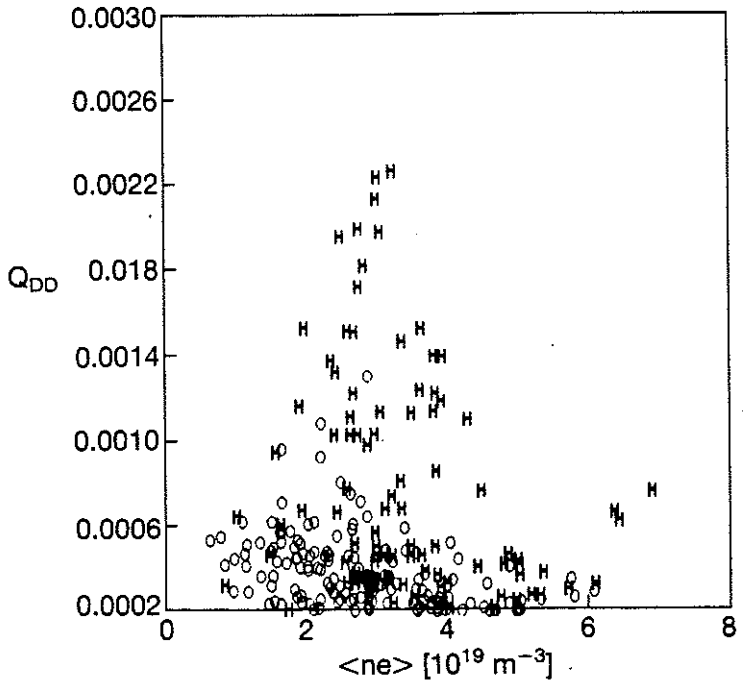

Fig.17. Measured Q_{DD} values averaged over 0.2 s as function of the volume averaged electron density $<n_e>$ for H-mode discharges (H) with currents between 3 and 5 MA and limiter discharges (O) with currents between 2 and 6.5 MA.

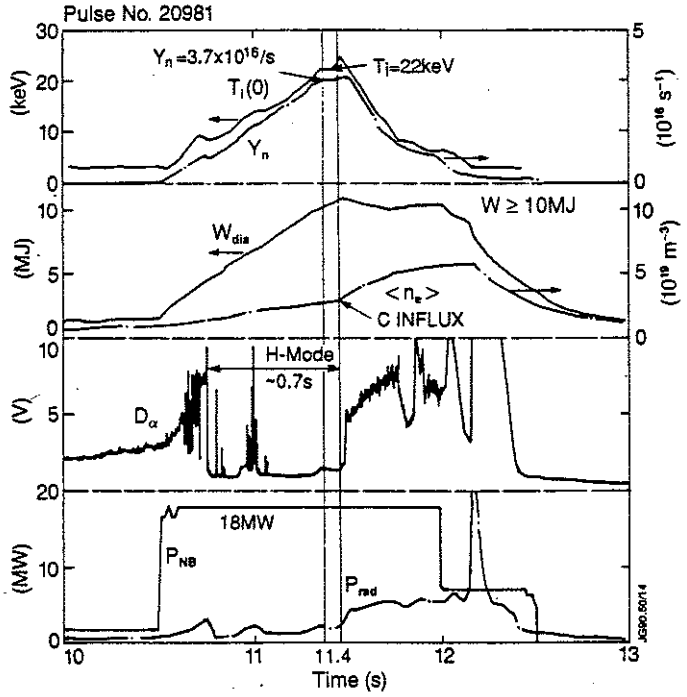

Fig.18. Time evolution of high fusion yield H-mode pulse #20981. From top to bottom are depicted the central ion temperature $T_i(0)$, the total neutron yield Y_n, the plasma diamagnetic energy W_{dia}, the volume averaged electron density $<n_e>$, the D_α intensity near the X-point, the neutral beam power P_{NB} and the radiated power losses P_{rad} as function of time. The large carbon influx at 11.5 s (marked by the second vertical line) is followed by a termination of the H-mode and an abrupt decrease in the high values of the fusion relevant parameters.

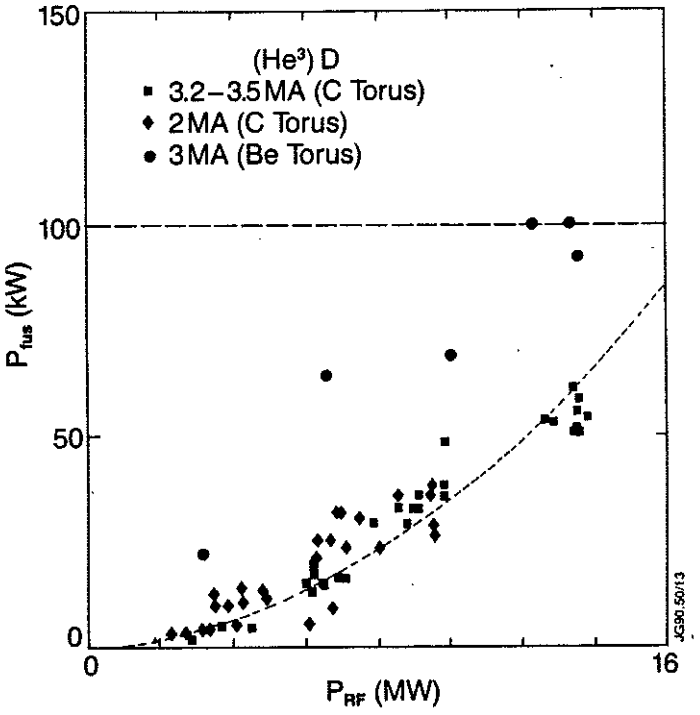

Fig.19. The measured fusion production P_{fus} in a deuterium plasma with ^{3}He minority as function of the ICRH power P_{RF}. The solid symbols (▪,$\hat{\nabla}$) are the fusion yields in a carbon vacuum vessel. The higher points (o) are obtained after the introduction of Be and reflect the improvement of n_D/n_e from ≤ 0.6 to ≥ 0.8.

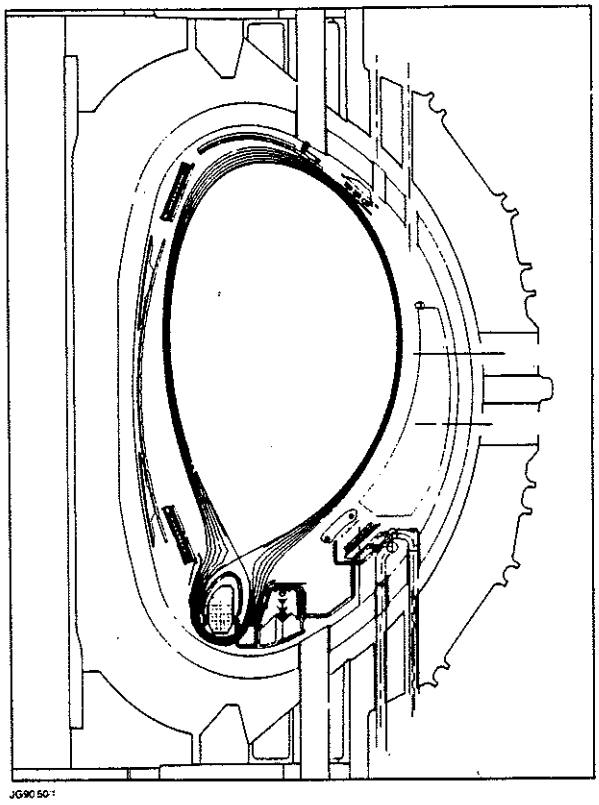

Fig.20. The proposed design of a new internally pumped divertor for JET. Cross-section of the magnetic field lines in the scrape-off layer and some principal new machine components.

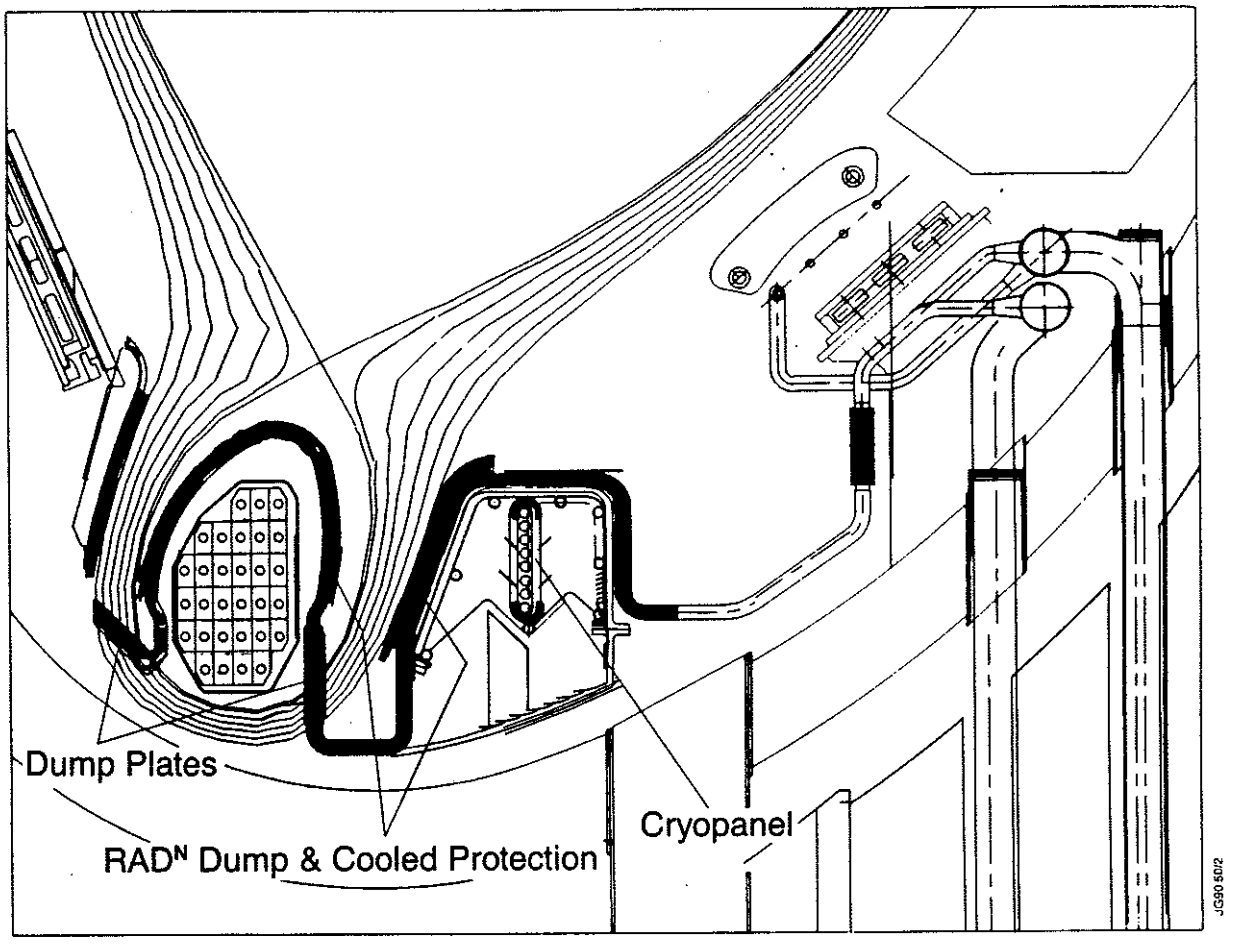

Fig.21. Divertor coil cross-section together with dump plates, radiation (RAD^N) dump- and cooled protection-plates and the cryo-panel unit in the lower part of the JET torus.

Table III : JET Programme in the New Phase

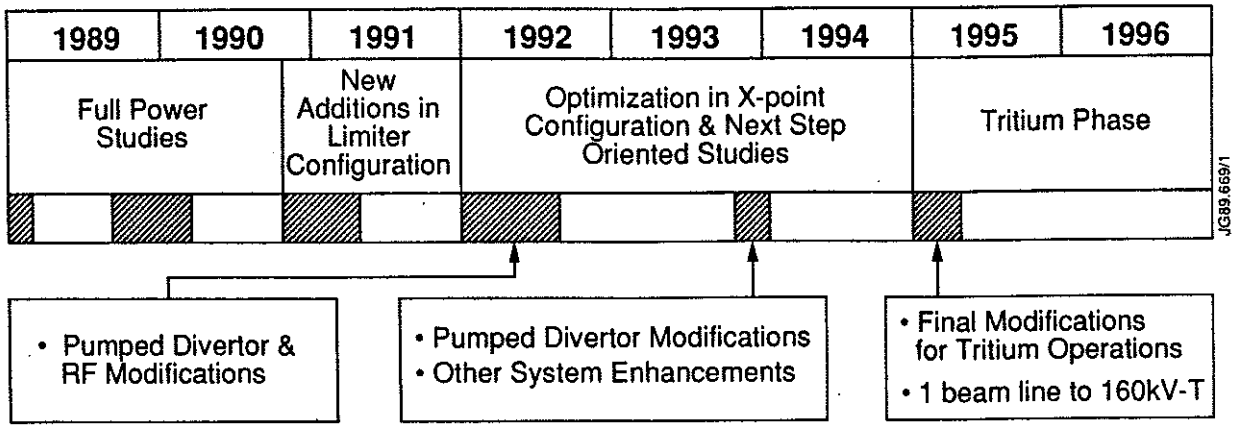

Fig.22. The JET Programme in the new phase upto the end of 1996.